A Model Of Pedestal Structure

J.D. Callen, University of Wisconsin, Madison, WI 53706-1609

C-Mod/NSTX Pedestal Workshop, PPPL, Princeton, NJ, September 7–8, 2010

Theses:

1) A comprehensive model for the pedestal structure can be developed[1] assuming paleoclassical plasma transport dominates throughout the pedestal.

2) Predictions are developed[1] for $dT_e/d\rho$, $n_e(\rho)$, density fueling effects, initial transport-limited height of $\beta_e^{\rm ped}$, $dT_i/d\rho$, $\Omega_t(\rho)$, charge-exchange effects on $\Omega_t(\rho)$ and resultant radial electric field $E_\rho(\rho)$ in the pedestal.

3) All the predictions agree (within ~ 2) with DIII-D 98889 pedestal data.[2]

4) Model provides interpretation of key transport properties that underlie QH-modes, EDA H-modes, I-modes and transport responses to RMPs.

5) Validation tests are suggested:[1] 4 fundamental, 4 secondary, 4 scenarios.

[1] J.D. Callen, "A Model of Pedestal Transport," report UW-CPTC 10-6, August 30, 2010, available via `http://www.cptc.wisc.edu`.

[2] J.D. Callen, R.J. Groebner, T.H. Osborne, J.M. Canik, L.W. Owen, A.Y. Pankin, T. Rafiq, T.D. Rognlien and W.M. Stacey, "Analysis of pedestal transport," Nuclear Fusion **50**, 064004 (2010).

Motivation: What Are Key Transport Issues For Pedestals?

- **How does the huge electron heat flux from core get carried through the low n_e, T_e pedestal? Answer: by making $|dT_e/d\rho|$ very large $\Longrightarrow$ T_e pedestal.**

  Conductive electron heat flow (Watts) through a flux surface (S) is $P_e \simeq n_e \chi_e S \left(-\dfrac{dT_e}{d\rho}\right)$.

  The needed T_e gradient in the pedestal is thus $\dfrac{1}{L_{Te}} \equiv -\dfrac{1}{T_e}\dfrac{dT_e}{d\rho} = \dfrac{P_e}{n_e T_e \chi_e S}$.

  $P_e \sim \dfrac{\overline{n_e T_e}\, V}{\tau_E}$ & $\tau_E \sim \dfrac{a^2}{\overline{\chi}_e}$ yields $\dfrac{a}{L_{Te}} \sim \dfrac{\overline{n_e T_e}}{n_e^{\rm ped} T_e^{\rm ped}} \gg 10$ if $\overline{\chi}_e \sim \chi_e^{\rm ped}$.

  Paleoclassical $\chi_e^{\rm pc}$ agreed with interpretive χ_e in 98889 pedestal[2] and $\chi_e^{\rm pc}(\text{ped}) \sim \overline{\chi}_e$.

- **How does the density build up so high with modest core fueling and mostly edge fueling (up steep pedestal density gradient!)? Answer: density pinch.**

  It has long been known that density pinches are important in H-mode pedestals.[3]
  Interpretive Stacey-Groebner analysis[4] indicates inward pinch nearly cancels diffusion.
  Paleoclassical model predicted density pinch and inferred diffusivity in 98889 pedestal.[2]

CONCLUSION: A complete pedestal structure model based on paleoclassical transport should be developed — for $n_e(\rho)$, $T_e(\rho)$, $\Omega_t(\rho)$ and $E_\rho(\rho)$.

---

[3] M.E. Rensink, S.L. Allen, A.H. Futch, D.N. Hill, G.D. Porter and M.A. Mahdavi, "Particle transport studies for single-null divertor discharges in DIII-D," Phys. Fluids B **5**, 2165 (1993).

[4] W.M. Stacey and R.J. Groebner, "Interpretation of particle pinches and diffusion coefficients in the edge pedestal of DIII-D H-mode plasmas," Phys. Plasmas **16**, 102504 (2009).

Outline

- **Key profile properties of DIII-D 98889 pedestal**[2]
- **Paleoclassical transport model**
- **Pedestal plasma transport equations**
- **Pedestal structure:**
  - **electron density profile**
  - **electron temperature profile**
  - **ion temperature profile**
  - **toroidal flow profile and radial electric field**
- **Discussion:**
  - **sources of error — in key data and paleoclassical theory**
  - **pedestal profile evolution into ELMs**
  - **interpretations of QH-modes, EDA H-modes and I-modes**
  - **interpretation of transport effects of RMPs**
- **Experimental validation tests**
- **Summary**

98889 Pedestals: ***Transport Quasi-equilibrium Will Be Studied***

- **LSN DIII-D 98889 discharge has:**[2]

  $P_{\rm NBI} \simeq 2.91$ **MW,**

  $P_{\rm OH} \simeq 0.3$ **MW,**

  $B_{\rm t0} \simeq 2$ **T,**

  $I \simeq 1.2$ **MA,**

  $q_{95} \simeq 4.4$**,**

  $a \simeq 0.77$ **m,**

  mid-plane half-radius $r_M \simeq 0.6$ **m,**

  low $n_e^{\rm ped}$**, high** $T_e^{\rm ped}$**.**

- **Transport question to be addressed is:**

  Can initial ($\sim$ 10 ms), transport-limited, quasi-equilibrium pedestal structure be predicted?

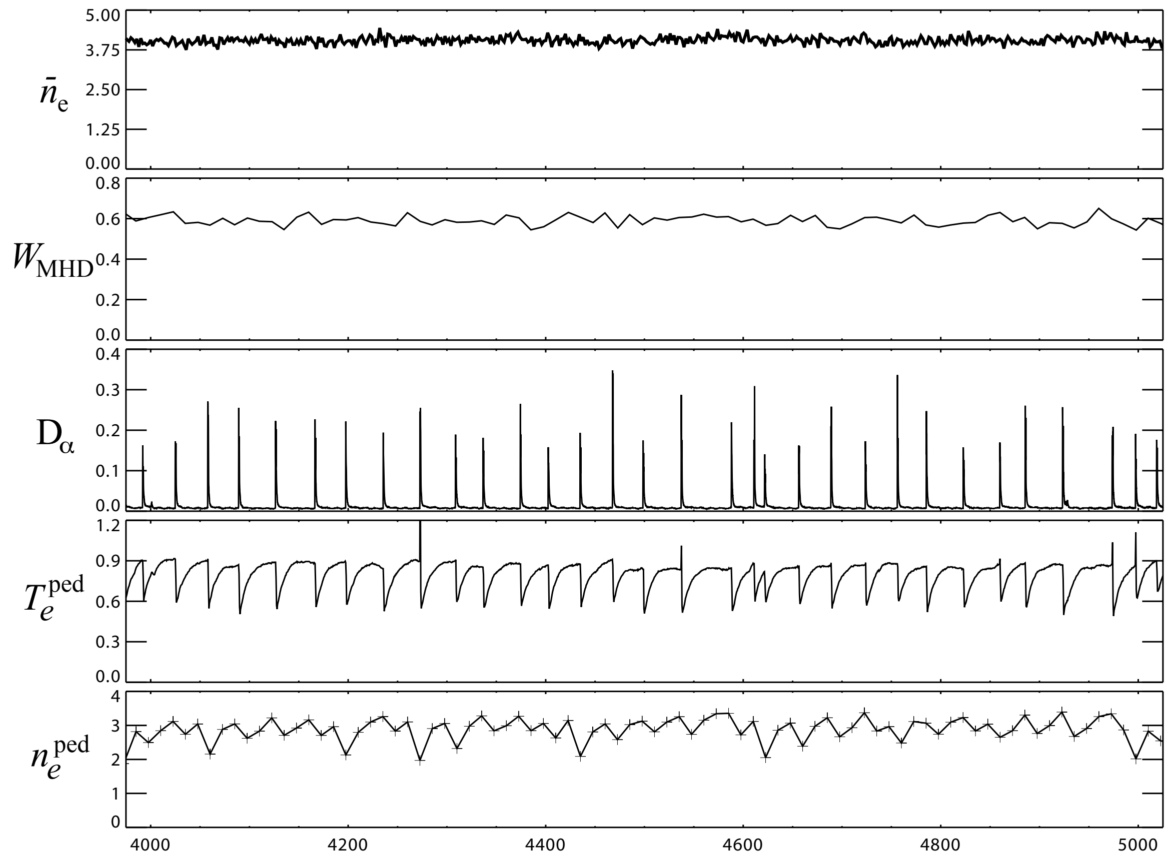

Figure 1: $\boldsymbol{T_e}$ and $\boldsymbol{n_e}$ profiles recover quickly ($\sim$ 10 ms) after ELM, then evolve slowly ($\sim$ 25 ms) to next ELM. Quasi-equilibrium profiles are obtained by binning 80-99 % data of ELM cycles, averaging over 4–5 s.[2]

Pedestal: ***Low Density LSN DIII-D 98889 Pedestal Is Studied***[2]

- **Experimental data is fit to tanh (n_e, T_e) & spline (T_i) profiles.**

- **Radial coordinate used is $\rho \equiv \sqrt{\Phi/\pi B_{t0}}$ with $\rho_N \equiv \rho/a$.**

- **Defined pedestal regions are:**

  I: core, $0.85 < \rho_N < 0.96$,
  pedestal "top" is at $\rho_t \simeq 0.96a$,
  II: top half, $0.96 < \rho_N < 0.98$,
  density mid-point is at $\rho_n \simeq 0.982a$,
  III: bottom half, $0.98 < \rho_N < 1.0$.

- **Key pedestal profile features:**

  n_e "aligned" with T_e profile,
  $dT_e/d\rho \simeq$ constant in pedestal,
  "top" of T_e pedestal hard to identify,
  $|dT_i/d\rho|$ is smallest gradient.

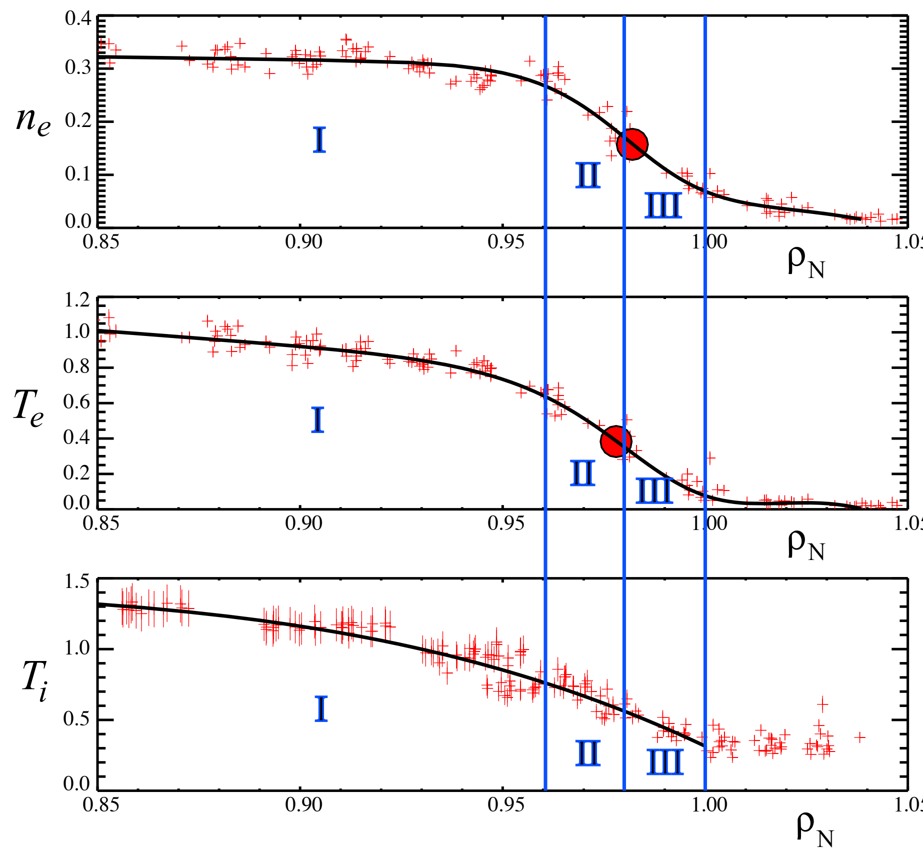

Figure 2: Edge profiles for n_e, T_e, and T_i are obtained by averaging Thomson and CER data over 80–99 % of average 33.53 ms between ELMs.[2] Lines show tanh & spline fits; red dots are fit symmetry points.

Paleoclassical Effects Occur In All Transport Channels

- *Density* of a species s (electrons and all ions — intrinsically ambipolar):[5]

$$\Gamma_{spc} \equiv -\frac{1}{V'}\frac{\partial}{\partial \rho}(V'\bar{D}_\eta n_{s0}) = -\bar{D}_\eta \frac{\partial n_{s0}}{\partial \rho} + n_{s0} V_{\rm pc}, \qquad \boxed{V_{\rm pc} \equiv -\frac{1}{V'}\frac{\partial}{\partial \rho}(V'\bar{D}_\eta) \sim -\frac{3\,\bar{D}_\eta}{2\,L_{Te}}.}$$

- *Electron heat transport* has a different transport operator:[5]

$$\langle \vec{\nabla}\cdot \vec{Q}_e^{\rm pc}\rangle = -\frac{M+1}{V'}\frac{\partial^2}{\partial \rho^2}\left(V'\bar{D}_\eta \frac{3}{2} n_e T_e\right), \quad \text{with} \quad M \simeq \frac{\lambda_e}{\pi R_0 q} \sim 0\text{–}5 \text{ in pedestal region.}$$

- *Ion heat transport* is similar[6] to density transport:

$$\Upsilon_{spc} \equiv -\frac{1}{V'}\frac{\partial}{\partial \rho}\left(V'\bar{D}_\eta \frac{3}{2} n_{i0} T_{i0}\right) = -\bar{D}_\eta \frac{\partial}{\partial \rho}\left(\frac{3}{2} n_{i0} T_{i0}\right) + \frac{3}{2} n_{i0} T_{i0} V_{\rm pc}.$$

- *Toroidal momentum radial transport* is similar[5] to density and ion heat transport ($L_t \equiv m_i n_{i0} \langle R^2 \Omega_t\rangle$, FSA plasma toroidal angular momentum density):

$$\Pi_{\rho\zeta} \equiv -\frac{1}{V'}\frac{\partial}{\partial \rho}(V'\bar{D}_\eta L_t) = -\bar{D}_\eta \frac{\partial L_t}{\partial \rho} + L_t V_{\rm pc}.$$

- **Pinch effects from $V_{\rm pc}$ are due to structure of paleo transport operators.**

[5] J.D. Callen, A.J. Cole, and C.C. Hegna, "Toroidal flow and radial particle flux in tokamak plasmas," Phys. Plasmas **16**, 082504 (2009).
[6] J.D. Callen, C.C. Hegna, and A.J. Cole, "Transport equations in tokamak plasmas," Phys. Plasmas **17**, 056113 (2010).

Key Paleoclassical Parameter Is Magnetic Field Diffusivity D_η

- Magnetic field diffusivity is induced by parallel neoclassical resistivity $\eta_\parallel^{\rm nc}$:

$$\boxed{D_\eta \equiv \frac{\eta_\parallel^{\rm nc}}{\mu_0} = \frac{\eta_0}{\mu_0}\frac{\eta_\parallel^{\rm nc}}{\eta_0},} \quad \text{in which reference diffusivity is} \quad \boxed{\frac{\eta_0}{\mu_0} \equiv \frac{m_e \nu_e}{\mu_0 n_e e^2} \simeq \frac{1400\, Z_{\rm eff}}{[T_e({\rm eV})]^{3/2}}\frac{\ln\Lambda}{17}.}$$

- Ratio of neoclassical to reference ($\perp$) resistivity is approximately (for 98889)

$$\boxed{\frac{\eta_\parallel^{\rm nc}}{\eta_0} \simeq \frac{\eta_\parallel^{\rm Sp}}{\eta_0} + \frac{\mu_e}{\nu_e},} \quad \text{with} \quad \underbrace{\frac{\eta_\parallel^{\rm Sp}}{\eta_0} \simeq \frac{\sqrt{2}+Z_{\rm eff}}{\sqrt{2}+13 Z_{\rm eff}/4}}_{\text{Spitzer}} \quad \text{and} \quad \underbrace{\frac{\mu_e}{\nu_e} \simeq \frac{4}{1+\nu_{*e}^{1/2}+\nu_{*e}}}_{\text{t.p. viscosity effect}}$$

- Basic scaling is $D_\eta \propto Z_{\rm eff}/T_e^{3/2}$ but viscosity effects due to large fraction of trapped particles ($f_t \simeq 0.7$) cause $\eta_\parallel^{\rm nc}/\eta_0$ to vary a lot in 98889 pedestal:

$$\frac{\eta_\parallel^{\rm nc}}{\eta_0} \simeq 0.4 \text{ (on separatrix)}, \sim 0.7\text{–}1.67 \text{ (at } \rho_n \simeq 0.982a), \sim 1.1\text{–}2.1 \text{ (at } \rho_{\rm t} \simeq 0.96a);$$

lower numbers are from $\epsilon \ll 1$ ONETWO formula, higher ones are approximation above.

- For simplicity of notation the geometrically effective D_η will be written as

$$\boxed{\bar{D}_\eta \equiv \frac{a^2}{\bar{a}^2} D_\eta,} \quad \text{in which} \quad \frac{a^2}{\bar{a}^2} \equiv \frac{1}{\langle R^{-2}\rangle}\left\langle \frac{|\vec{\nabla}\rho|^2}{R^2}\right\rangle \simeq 1.6 \text{ in 98889 pedestal.}$$

Pedestal Plasma Transport Equations

- **Assumptions are made in order to develop this pedestal structure model:**

  1) Paleoclassical transport dominates density and electron temperature transport in the pedestal, but anomalous transport is dominant from top of pedestal into the core.

  2) Electron heating in the pedestal is small; heat mostly just flows out through pedestal.

  3) Density is fueled from the edge recycling ion source, perhaps plus NBI core fueling.

- **Thus, equilibrium electron density and energy conservation equations are:**

$$\langle \vec{\nabla} \cdot (\vec{\Gamma}^{\rm pc} + \vec{\Gamma}^{\rm an}) \rangle = \langle S_n \rangle \quad \Longrightarrow \quad -\frac{1}{V'}\frac{d^2}{d\rho^2}(V'\bar{D}_\eta n_e) + \frac{1}{V'}\frac{d}{d\rho}(V'\Gamma^{\rm an}) = \langle S_n(\rho) \rangle,$$

$$\langle \vec{\nabla} \cdot (\vec{q}_e^{\,\rm pc} + \vec{q}_e^{\,\rm an} + \tfrac{5}{2}T_e\vec{\Gamma}) \rangle = 0 \quad \Longrightarrow -\frac{M+1}{V'}\frac{d^2}{d\rho^2}\left(V'\bar{D}_\eta \frac{3}{2} n_e T_e\right) + \frac{1}{V'}\frac{d}{d\rho}\left[V'(\Upsilon_e^{\rm an} + \frac{5}{2}T_e\Gamma)\right] = 0.$$

- **Neglecting anomalous density transport in the pedestal, the density equation can be integrated from ρ to the separatrix ($\rho = a$) to yield**

$$-\left[\frac{d}{d\rho}(V'\bar{D}_\eta n_e)\right]_\rho = \dot{N}(\rho), \qquad \text{\#/s of electrons flowing outward through the } \rho \text{ surface.}$$

- **Neglecting anomalous electron heat xport in pedestal and integrating yields**

$$-\left[\frac{d}{d\rho}\left(V'\bar{D}_\eta \frac{3}{2} n_e T_e\right)\right]_\rho = \hat{P}_e(\rho), \quad \text{effective electron power flow (W) through } \rho \text{ surface.}$$

Pedestal Electron Density Profile

- **Integrating density flow equation from ρ surface to separatrix ($\rho = a$) yields**

$$n_e(\rho)\,\bar{D}_\eta(\rho)\,V'(\rho) \;=\; n_e(a)\,\bar{D}_\eta(a)V'(a) \;+\; \textstyle\int_\rho^a d\hat{\rho}\,\dot{N}_e(\hat{\rho}).$$

- **However, fueling effect from $\dot{N}$ is often small:**

$$\frac{\int_{\rho_n}^a d\hat{\rho}\,\dot{N}_e(\hat{\rho})}{[n_e \bar{D}_\eta V']_{\rho_n}} \simeq \frac{(a-\rho_n)\,\dot{N}_e[(a+\rho_n)/2]}{n_e(\rho_n)\,\bar{D}_\eta(\rho_n)\,V'(\rho_n)} \simeq 0.04 \ll 1 \qquad \text{for 98889 pedestal.}$$

- **Neglecting fueling and variation of V', integrated density equation becomes**

$$\boxed{n_e(\rho)\,\bar{D}_\eta(\rho) \simeq \text{constant} \quad \Longrightarrow \quad n_e(\rho) \simeq n_e(a)\,\frac{\bar{D}_\eta(a)}{\bar{D}_\eta(\rho)}, \quad \text{within the pedestal,}}$$

which is density profile needed for outward diffusive flux to be cancelled by pinch flow.

- **Density profile $\sim 1/\bar{D}_\eta \sim f(T_e)$ leads to "aligned" n_e, T_e profiles.**

In 98889 pedestal $n_e(\rho_n)/n_e(a) \simeq 2.14$ whereas model predicts $n_e(\rho_n)/n_e(a) \simeq 1.9$–$4.4$.

- **Estimate fueling effects with $\dot{N}_e \simeq \dot{N}_e(a)e^{-(a-\rho)/\lambda_n}$ and assume $\lambda_n > a - \rho$:**

$$\boxed{n_e(\rho)\,\bar{D}_\eta(\rho)\,V'(\rho) \simeq n_e(a)\,\bar{D}_\eta(a)\,V'(a) + \dot{N}_e(a)\,(a-\rho),} \qquad \text{which shifts } n_e \text{ profile}$$

outward relative to T_e profile — like in JET/DIII-D comparison experiments?[7]

[7] M.N.A. Beurkens, T.H. Osborne et al., "Pedestal width and ELM size identity studies in JET and DIII-D ...," PPCF **51**, 124051 (2009).

Pedestal Electron Temperature Profile

- **Using density flow equation in electron energy flow equation and neglecting fueling effect [$(3/2)\dot{N}_e T_e/\hat{P}_e \sim 0.025$ in 98889] yields T_e gradient prediction:**

$$\boxed{-\frac{dT_e}{d\rho} = \frac{\hat{P}_e(\rho)}{(3/2)\,[V'\bar{D}_\eta\, n_e]} \simeq \text{ constant,}}$$

because $\hat{P}_e$ & $[V'\bar{D}_\eta n_e]$ are $\simeq$ constant in pedestal.

- **This predicts electron temperature gradient scale length ("pedestal width") at the density mid-point is (98889 data[2] indicates $L_{Te}/a \simeq 0.02$):**

$$\boxed{\frac{L_{Te}}{a} \equiv \left[-\frac{a}{T_e}\frac{dT_e}{d\rho}\right]^{-1}_{\rho_n} \simeq \frac{(3/2)[V'\bar{D}_\eta\, n_e]_{\rho_n} T_e(\rho_n)}{a\,\hat{P}_e(\rho_n)}} \simeq 0.033\text{–}0.066, \text{ does not depend on } \rho_*.$$

- **Since $\eta_e \gtrsim 2 \gg \eta_{e,\mathrm{crit}} \simeq 1.2$ at top of pedestal, we are in "saturated" ETG regime where anomalous electron heat transport can be represented by[2,8]**

$$\chi_e^{\rm ETG} \simeq f_\# \chi_e^{\rm gB} \equiv f_\# \frac{\rho_e}{L_{Te}}\frac{T_e}{eB_{\rm t0}} \simeq 0.075\, f_\# \frac{[T_e(\mathrm{keV})]^{3/2}}{L_{Te}(\mathrm{m})\, B_{\rm t0}^2(\mathrm{T})^2}\ \mathrm{m}^2/\mathrm{s}, \qquad \text{with}^{2,8}\ f_\# \simeq 1.4\text{–}3.$$

- **Estimate the pedestal height by equating the ETG heat flow $\Upsilon_{eETG} \simeq -n_e\chi_e^{\rm ETG} dT_e/d\rho$ to the paleoclassical electron heat flow to obtain**

$$\boxed{\beta_e^{\rm ped} \equiv \frac{n_e^{\rm ped}T_e^{\rm ped}}{B_{\rm t0}^2/2\mu_0} \sim \frac{3\sqrt{2}}{\pi f_\#}\,\frac{\eta_\parallel^{\rm nc}}{\eta_0}\,\frac{L_{Te}}{R_0 q}} \simeq 0.0035\text{–}0.007 \text{ prediction vs. } 0.002 \text{ in 98889 pedestal.}$$

[8] F. Jenko et al., "Gyrokinetic turbulence under near-separatrix or nonaxisymmetric conditions," Phys. Plasmas **16**, 055901 (2009).

Pedestal Ion Temperature Profile

- Ion heat transport in H-mode pedestals is apparently a complicated mix of

  comparable neoclassical and paleoclassical transport throughout the pedestal,
  transition to ITG-driven anomalous transport in the core, and
  kinetic effects in the bottom half of the pedestal, near the separatrix.

- Neglecting anomalous ion heat transport and kinetic effects, and integrating the ion energy equation as was done for the n_e and T_e equations yields

$$-\frac{dT_i}{d\rho} \simeq \frac{P_i(\rho)/V'}{(3/2)n_i\bar{D}_\eta + n_i\chi_i^{\rm nc}}, \qquad \boxed{\left.\frac{L_{Ti}}{a}\right|_{\rho_n} \equiv \left[-\frac{a}{T_i}\frac{dT_i}{d\rho}\right]_{\rho_n}^{-1} \simeq \frac{[(3/2)\bar{D}_\eta + \chi_i^{\rm nc}]_{\rho_n} n_i(\rho_n)\, T_i(\rho_n)}{a\, P_i(\rho_n)/V'}.}$$

- Since $n_i\bar{D}_\eta$ and $\chi_i^{\rm nc}$ are nearly constant in the pedestal, the ion temperature gradient $dT_i/d\rho$ is also approximately constant in the pedestal.

- For the 98889 pedestal $[L_{Ti}/a]_{\rho_n} \simeq 0.06$ versus prediction of 0.12–0.21 — it seems that both the $\chi_i^{\rm nc}$ and $\chi_i^{\rm pc}$ theoretical values are a bit too large?[2]

- Determining "top" of T_i pedestal is problematic because multiple ion heat transport processes are involved and ITG transport is likely near threshold.

Pedestal Toroidal Flow Profile And Radial Electric Field

- Poloidal ion flow should be predicted by neo theory: $V_{\mathrm{p}i} \simeq (k_i/q_i B_{\mathrm{t}0})(dT_i/d\rho)$.
- Equation for plasma toroidal angular momentum has been derived recently.[5]
- Neglecting 3D and microturbulence effects, but including paleoclassical transport and charge-exchange momentum losses $\langle \vec{e}_\zeta \cdot \vec{S}_m \rangle \simeq -\nu_{\mathrm{cx}} L_{\mathrm{t}}$ yields

$$-\frac{1}{V'}\frac{d^2}{d\rho^2}[V'\bar{D}_\eta L_{\mathrm{t}}] \simeq -\nu_{\mathrm{cx}} L_{\mathrm{t}}, \quad \text{in which} \quad L_{\mathrm{t}} \equiv m_i n_i \langle R^2 \rangle \Omega_{\mathrm{t}} \text{ is total plasma ang. mom.}$$

- Neglecting charge-exchange losses and analyzing as for density profile yields[1]

$$\boxed{\Omega_{\mathrm{t}}(\rho) \simeq \text{constant} \quad \Longrightarrow \quad \Omega_{\mathrm{t}}(\rho) \simeq \Omega_{\mathrm{t}}(a) \quad \text{in pedestal,}} \quad \text{as found in 98889 pedestal.}^{9}$$

- Adding charge exchange effects and again assuming $\lambda_n > a - \rho$ yields[1]

$$\Omega_{\mathrm{t}}(\rho) \simeq \Omega_{\mathrm{t}}(a)\,[1 - (a-\rho)\lambda_n \nu_{\mathrm{cx}}(a)/\bar{D}_\eta(a)], \qquad \text{linearly increasing } \Omega_{\mathrm{t}} \text{ with } \rho.^{10,11}$$

- Adding ripple effects reduces Ω_{t} in pedestal $\propto \delta B_N^2$, as observed in JET.[7]
- Electric field is determined from radial force balance once Ω_{t} is known:

$$E_\rho = |\vec{\nabla}\rho| \left(\Omega_{\mathrm{t}} \psi_{\mathrm{p}}' + \frac{1}{n_i q_i}\frac{dp_i}{d\rho} - \frac{k_i}{q_i}\frac{dT_i}{d\rho} \right) \simeq |\vec{\nabla}\rho| \frac{1}{n_i q_i}\frac{dp_i}{d\rho} \quad \text{since } \Omega_{\mathrm{t}} \text{ and } \frac{dT_i}{d\rho} \text{ are small.}$$

---

[9] W.M. Stacey, "The effects of rotation, electric field, and recycling neutrals on determining the edge pedestal density ...," PoP **17**, 052506 (2010).
[10] J.S. deGrassie, J.E. Rice, K.H. Burrell. R.J. Groebner, and W.M. Solomon, "Intrinsic rotation in DIII-D," PoP **14**, 056115 (2007).
[11] T. Pütterich et al., "Evidence for Strong Inversed Shear of Toroidal Rotation at the Edge-Transport Barrier in AUG," PRL **102**, 025001 (2009).

Discussion I: Sources Of Error And Pedestal Evolution

- **Determination of $D_\eta \propto f(\nu_{*e}) Z_{\rm eff}/T_e^{3/2}$ is critical but (factors $\lesssim 2$):**

  $Z_{\rm eff}$ is often assumed to be constant in pedestal[2] but should decrease toward separatrix.

  A better formula for $\eta_\parallel^{\rm nc}$ is needed than the $\epsilon \ll 1$ formula used in ONETWO.

  In paleoclassical theory D_η should be multiplied by fraction of $\psi_{\rm p}$ due to local $\langle \vec{J}\cdot\vec{B}\rangle$.

- **The $\beta_e^{\rm ped}$ prediction here is just for the initial, transport-limited pedestal height immediately after L-H transition or an ELM:**

  Pedestal should reach this state in $\tau \sim (2L_{Te})^2/\bar{D}_\eta$ ($\sim$ few ms for 98889 parameters[2]).

  Then, top of pedestal moves radially inward as core plasma re-equilibrates — but n_e and T_e profiles in the pedestal should remain fixed on the longer "global" τ_E time scale.

  Continuing growth and inward spreading of top of T_e profile eventually violates peeling-ballooning (PB) instability boundary and precipitates an ELM.

  If electron heat flow through pedestal $\hat{P}_e$ is too large, P-B limit could be exceeded before this "quasi-equilibrium" $\beta_e^{\rm ped}$ is reached — then T_e would rise linearly between ELMs.

  In this situation one would obtain more frequent Type I ELMs, perhaps accompanied by Type II ELMs if high-n ballooning limit is exceeded in bottom half of the pedestal.

Discussion II: Interpretations Of ELM-free Pedestals

- **Plasma should revert to L-mode if microturbulence-induced anomalous transport fluxes exceed paleoclassical ones, i.e., for**

  $D^{\rm an} > D^{\rm pc}_{\rm eff} \simeq f_D D_\eta$ **where** f_D **(**~ 0.1 **in 98889**^{2}**) is degree of diffusion reduction by pinch,**
  $\chi_e^{\rm an} > \chi_e^{\rm pc} \simeq (3/2)(M+1)D_\eta$ **for electron heat transport.**

- **However, since** $D^{\rm pc}_{\rm eff}/\chi_e^{\rm pc} \sim f_D/M \ll 1$ **(ratio is** ~ 0.03 **in 98889) an "intermediate" regime with** T_e **pedestal but less** n_e **pedestal can exist because:**

  Microturbulence-induced anomalous transport typically has $D^{\rm an} \sim \chi_e^{\rm an}$**.**
  For $D^{\rm an} > D^{\rm pc}_{\rm eff}$ **but** $\chi_e^{\rm an} < \chi_e^{\rm pc}$**,** $|dn_e/d\rho|$ **is reduced but** $|dT_e/d\rho|$ **does not change.**

- **Possible ELM-free modes of operation where this could be occuring are:**

  QH-modes in DIII-D with EHOs providing $D^{\rm an} > D^{\rm pc}_{\rm eff}$**,**
  EDA H-modes in C-Mod with EDAs providing $D^{\rm an} > D^{\rm pc}_{\rm eff}$**, and**
  I-modes in C-Mod with "moderate" microturbulence causing $D^{\rm an} > D^{\rm pc}_{\rm eff}$ **but** $\chi_e^{\rm an} < \chi_e^{\rm pc}$**.**

- **Effects of RMPs on pedestal can also be interpreted with this model:**

  Key RMP effects:[12] $n_e(a)\downarrow$ **and** $\max\{|dT_e/d\rho|\}\uparrow$ **by factors of 2; but** $T_e^{\rm ped} \simeq$ **constant.**
  For separatrix $n_e(a)\downarrow$ **model predicts** $|dT_e/d\rho|\uparrow$**,** $\beta_e^{\rm ped}\downarrow$ **(by same factor);** $T_e^{\rm ped} \simeq$ **const.**

[12] T.E. Evans et al., "Edge stability and transport control with resonant magnetic perturbations in collisionless ...," Nature Physics **2**, 419 (2006).

Suggested Experimental Validation Tests I

- **This new pedestal structure model is quantitatively consistent (factor $\sim$ 2) with 98889 data[2] and qualitatively agrees with pedestal evolution and ELM-free H-mode regimes. However, it needs to be validated by testing:**

  its scaling properties, over wider data sets and its ELM-free mode predictions.

- **Like neoclassical transport, no phenomenology underlies paleoclassical transport that can be tested experimentally — but resistivity is neoclassical.**

- **The most <u>fundamental tests</u> of this new pedestal structure model are:**

  #1: When fueling effects are negligible, is $n_e(\rho)\,\bar{D}_\eta(\rho) \simeq$ constant within the pedestal?

  #2: Is T_e gradient approximately constant in the pedestal at the predicted magnitude?

  #3: Does "pedestal width" $[L_{Te}/a]_{\rho_n}$ at pedestal density mid-point scale as predicted? When other parameters are held constant, the T_e gradient scale length should increase slightly with non-cirularity ($\propto V'$), and with electron density n_e and temperature T_e at the mid-point of the pedestal density profile (ρ_n). In addition, it should decrease with increased conductive electron heat flow $\hat{P}_e$ at constant $n_e(\rho_n)$.

  #4: Can it be shown that long wavelength ($k_\perp \varrho_i \lesssim 1$) fluctuations within the pedestal do not contribute significantly to plasma transport there?

Suggested Experimental Validation Tests II

- Secondary tests that result from added effects are:

  #1: Does the top of the density pedestal occur where $d\ln\bar{D}_\eta/d\rho \lesssim 1/a$ with a height predicted by the minimum of $n_e(a)\bar{D}_\eta(a)/\bar{D}_\eta(\rho_t)$ or $\max\{n^{\rm ped}\} \sim \dot{N}a/\bar{D}_\eta V'$?

  #2: Are edge fueling effects on the pedestal n_e profile as predicted? And does this shift the pedestal n_e profile outward relative to the T_e profile as ϱ_* is decreased in DIII-D?[7]

  #3: Is the "initial" quasi-stationary pedestal electron pressure height predicted by $\beta_e^{\rm ped}$? And at top of the T_e pedestal do ETG-type fluctuations cause $\chi_e^{\rm ETG} \gtrsim \chi_e^{\rm pc}$ there?

  #4: When cx effects are negligible, is total plasma toroidal rotation frequency $\Omega_t \simeq V_t/R$ $\simeq$ constant in pedestal at its separatrix value $\Omega_t(a)$? Are cx effects on $\Omega_t(\rho)$ as predicted?

- Improvement scenario predictions for how to reduce $d\beta^{\rm ped}/d\rho$ and/or the pedestal height $\beta_e^{\rm ped}$ to avoid P-B ELM stability boundary are:

  #1: Reduce the pedestal height by reducing the electron separatrix density $n_e(a)$ for a given $\hat{P}_e$ (via more pumping or divertor structure) — as apparently occurs with RMPs?

  #2: Reduce the pedestal T_e gradient by reducing $\hat{P}_e/V'$ with larger V' (via more highly shaped plasmas) and/or by reducing $\hat{P}_e$ (e.g., via larger Q_{ei} at higher n_e).

  #3: Add a small density flux in pedestal (via controlled fluctuations or RF waves resonant there?) — as apparently occurs in QH-modes, EDA H-modes and I-modes.

  #4: Prevent pressure increase and inward growth of the T_e pedestal "top" by decreasing n_e at the pedestal top via reducing $n_e(a)$ (via external pumping?) on the τ_E time scale?

Some Specific Tests Are Suggested For C-Mod and NSTX

- **Some areas where C-Mod could make unique validation contributions are:**

  Fundamental #1, #2: Do n_e and $dT_e/d\rho$ scale as predicted for various heating methods?

  Secondary #2, #4: Do atomic physics effects affect n_e, Ω_t pedestal profiles as predicted?

  Secondary #3: Does $\beta_e^{\rm ped}$ prediction explain C-Mod $\alpha \sim R_0 q^2 \, d\beta/d\rho$ pedestal scaling?

  Scenario #3: Do EDA H-modes and I-modes have $D^{\rm an} > D_{\rm eff}^{\rm pc}$ but $\chi_e^{\rm an} < \chi_e^{\rm pc}$?

- **Some areas where NSTX could make unique validation contributions are:**

  Fundamental #1, #2, #3: Does $D_\eta \propto \eta_\parallel^{\rm nc}$ predict effects with/without Li walls?

  Fundamental #4: Do $k_\perp \varrho_i \lesssim 1$ fluctuations cause negligible transport at low n_e, T_e?

  Secondary #2, #4: Do atomic physics effects affect n_e, Ω_t pedestal profiles as predicted?

  Secondary #3: Do ETG fluctuations cause T_e transport at top of pedestal but not in it?

Summary

- **Key predictions of this paleoclassical-based pedestal structure model are:**

  $|dT_e/d\rho| \propto \varrho_*^0$ increases until electron heat flow can be carried out through pedestal.

  The n_e profile adjusts to minimize net paleoclassical density transport (D_η vs. $V_{\rm pc}$).

  Plasma toroidal rotation $\Omega_{\rm t}(\rho)$ is nearly constant at separatrix value for small cx effects.

- **"First round" tests of this model have found:**

  agreement with 98889 pedestal data[2] to within a factor ~ 2,

  plausible pedestal evolution scenarios for precipitating Type I and II ELMs, and

  interpretations of ELM-free H-modes via slightly increased $D^{\rm an}$ or reduced $n_e(a)$.

- **Many experimental validation tests have been suggested: 4 fundamental, 4 secondary and 4 improvement scenarios.**

- **Additional notes:**

  Achieving control of density buildup in H-mode pedestals (via scenarios #1, #3 or #4?) is a desirable goal. It may be critical for ITER to heat a low n_e H-mode startup plasma to fusion burning conditions before adding density to increase fusion power output.

  Paleoclassical transport is a minimum transport level; adding other transport processes weakens the pedestal gradients (particularly of density) and increase its width.

Regime: ***Paleoclassical Transport Likely Dominates At Low T_e***

- **Since $D_\eta \propto \eta \propto 1/T_e^{3/2}$, $\chi_e^{\rm pc}$ in the confinement region (I) is typically**

$$\chi_{eI}^{\rm pc} \sim \frac{Z_{\rm eff}[\bar{a}({\rm m})]^{1/2}}{[T_e({\rm keV})]^{3/2}}\,\frac{\rm m^2}{\rm s} \;\gtrsim\; 1\ {\rm m^2/s}\ \text{for}\ T_e \lesssim 2\ {\rm keV}.$$

- **Microturbulence-induced transport usually has a gyroBohm scaling:**

$$\text{ITG, DTE:}\ \ \chi_e^{\rm gB} \equiv f_\# \frac{\varrho_s}{a}\frac{T_e}{eB} \simeq 3.2 f_\# \frac{[T_e({\rm keV})]^{3/2} A_i^{1/2}}{\bar{a}({\rm m})\,[B({\rm T})]^2}\,\frac{\rm m^2}{\rm s} \;\gtrsim\; 1\ {\rm m^2/s}\ \text{for}\ T_e \gtrsim 0.5\ {\rm keV}/f_\#^{2/3},$$

in which $f_\#$ is a threshold-type factor that depends on magnetic shear, T_e/T_i, ν_{*e} etc.

- **Thus, paleoclassical electron heat transport is likely dominant at low T_e:**

$$T_e \lesssim \boxed{T_e^{\rm crit} \equiv [B({\rm T})]^{2/3}[\bar{a}({\rm m})]^{1/2}/(3f_\#)^{1/3}\ {\rm keV}} \sim 0.6\text{–}2.4\ {\rm keV}\ \ (f_\# \sim 1/3),\ \text{present expt.}$$

- **In DIII-D the electron temperature T_e in the H-mode pedestal ranges from about 100 eV at the separatrix to about 1 keV at top of pedestal**

$\Longrightarrow$ **paleoclassical $\chi_e^{\rm pc}$ is likely to be dominant in DIII-D H-mode pedestal region.**

- **In ITER $T_e^{\rm crit} \sim 3.5$–5 keV $\Longrightarrow$ paleoclassical may be dominant for ITER ohmic startup and in the pedestal region?**

Paleoclassical Model Is Result Of Coordinate Transformation

- **Background:**

  Transport codes use toroidal-flux-based coordinates nearly fixed to lab coordinates.

  But particle guiding centers are fixed to poloidal flux via $p_{g\zeta} = mRv_\parallel - q\psi_p$ conservation.

  Thus, drift-kinetic, gyrokinetic and plasma transport equations must be transformed[13] from laboratory to poloidal magnetic flux (ψ_p) coordinates.

  Poloidal flux surfaces ψ_p move relative to toroidal surfaces ψ_t at the $\mathcal{O}\{\delta^2\}$ magnetic diffusion rate — diffuse because of plasma resistivity and advect because of ECCD etc.

  Guiding centers of particles diffuse and advect radially along with the poloidal flux ψ_p.[14]

- **Paleoclassical transport model[15,16] results from[14] transforming drift-kinetic equation from lab to poloidal flux coordinates, $\partial f/\partial t|_{\vec{x}} \Longrightarrow \partial f/\partial t|_{\psi_p}$ etc.**

- **This transformation results in addition[14–16] of a second order diffusive-type paleoclassical operator $\mathcal{D}\{f\}$ to the right side of the drift-kinetic equation.**

- **Paleoclassical transport operator $\mathcal{D}$ is not purely diffusive because it represents direct $\mathcal{O}\{\delta^2\}$ process; particles carried on diffusing ψ_p, $\langle \Delta x_{\psi_p}\rangle/\Delta t = 0$.**

---

[13] R.D. Hazeltine, F.L. Hinton, and M.N. Rosenbluth, "Plasma transport in a torus of arbitrary aspect ratio," Phys. Fluids **16**, 1645 (1973).
[14] J.D. Callen, Phys. Plasmas **14**, 040701 (2007); **14**, 104702 (2007); **15**, 014702 (2008).
[15] See `http://homepages.cae.wisc.edu/~callen/paleo` for an annotated list of publications about the paleoclassical transport model.
[16] J.D. Callen, "Paleoclassical transport in low-collisionality toroidal plasmas," Phys. Plasmas **12**, 092512 (2005).

Transformed Density Equation Includes Paleoclassical Effects

- FSA paleoclassical density transport operator $\mathcal{D} \sim \mathcal{O}\{\delta^2\}$ is[5,6]

$$\langle \mathcal{D}\{n_0\}\rangle \equiv -\underbrace{\dot{\rho}_{\psi_p}\frac{\partial n_0}{\partial \rho}}_{\psi_p \text{ advection}} + \underbrace{\langle \vec{\nabla}\cdot n_0 \vec{u}_G\rangle}_{\psi_t \text{ advection}} + \underbrace{\frac{1}{V'}\frac{\partial^2}{\partial \rho^2}(V'\bar{D}_\eta n_0)}_{\text{transport}}, \qquad \dot{\rho}_{\psi_p} \equiv \frac{\dot{\psi}_p}{\psi_p'}, \qquad \bar{D}_\eta \equiv \frac{D_\eta}{\bar{a}^2},$$

$$D_\eta \equiv \frac{\eta_\parallel^{\rm nc}}{\mu_0} \text{ (magnetic diffusivity)}, \quad \frac{1}{\bar{a}^2} \equiv \frac{1}{\langle R^{-2}\rangle}\left\langle \frac{|\vec{\nabla}\rho|^2}{R^2}\right\rangle \simeq \frac{1}{a^2}, \quad \langle \vec{\nabla}\cdot\vec{u}_G\rangle = \frac{1}{V'}\frac{\partial V'}{\partial t}\bigg|_\rho .$$

- Including transformation effects, FSA density equation can be written as

$$\boxed{\frac{1}{V'}\frac{\partial}{\partial t}\bigg|_{\psi_p}(V'n_0) + \underbrace{\dot{\rho}_{\psi_p}\frac{\partial n_0}{\partial \rho}}_{\psi_p \text{ advection}} + \underbrace{\frac{1}{V'}\frac{\partial}{\partial \rho}(V'\Gamma)}_{\text{transport}} = \underbrace{\langle \bar{S}_n\rangle}_{\text{sources}},}$$

$V'n_0$ is # particles between ρ and $\rho + d\rho$ surfaces, an adiabatic plasma property.

- The total $\mathcal{O}\{\delta^2\}$ particle flux for each species is:

$$\boxed{\Gamma \equiv \langle \vec{\Gamma}\cdot\vec{\nabla}\rho\rangle = \Gamma^a + \Gamma^{na} + \Gamma^a_{\rm pc} = \langle\, [\, \underbrace{n_0(\bar{\vec{V}}_2 - \vec{u}_G)}_{\text{collisional}} + \underbrace{\overline{\tilde{n}_1 \tilde{\vec{V}}_1}}_{\text{fluctuations}}\,]\cdot\vec{\nabla}\rho\,\rangle \underbrace{- \frac{1}{V'}\frac{\partial}{\partial\rho}(V'\bar{D}_\eta n_0)}_{\text{paleoclassical}}.}$$

- Paleoclassical particle flux has diffusive and pinch ($V_{\rm pc}$) components:

$$\Gamma^a_{\rm pc} \equiv -\frac{1}{V'}\frac{\partial}{\partial \rho}(V'\bar{D}_\eta n_0) = -\bar{D}_\eta\frac{\partial n_0}{\partial \rho} + n_0 V_{\rm pc}, \quad \text{with} \quad V_{\rm pc} \equiv -\frac{1}{V'}\frac{\partial}{\partial\rho}(V'\bar{D}_\eta) \sim -\frac{3\,\bar{D}_\eta}{2\,L_{Te}}.$$